Genome-Wide Analysis of Yield in Europe: Allelic Effects Vary with Drought and Heat Scenarios[1][OPEN]

Emilie J. Millet, Claude Welcker, Willem Kruijer, Sandra Negro, Aude Coupel-Ledru, Stéphane D. Nicolas, Jacques Laborde, Cyril Bauland, Sebastien Praud, Nicolas Ranc, Thomas Presterl, Roberto Tuberosa, Zoltan Bedo, Xavier Draye, Björn Usadel, Alain Charcosset, Fred Van Eeuwijk, and François Tardieu*

INRA, Laboratoire d'Ecophysiologie des Plantes sous Stress Environnementaux, 34060 Montpellier, France (E.J.M., C.W., A.C.-L., F.T.); Biometris — Applied Statistics, Department of Plant Science, Wageningen University, 6700AA Wageningen, Netherlands (W.K., F.V.E.); INRA, UMR 0320 / UMR 8120 Génétique Quantitative et Evolution, 91190 Gif-sur-Yvette, France (S.N, S.D.N., C.B., A.C.); INRA, SMH Maïs, Centre de recherche de Bordeaux Aquitaine, 40390 Saint-Martin-De-Hinx, France (J.L.); Centre de Recherche de Chappes, Biogemma, 63720 Chappes, France (S.P.); Syngenta France SAS, 12, Chemin de l'Hobit, BP 27, 31790, Saint-Sauveur, France (N.R.); KWS Saat SE, 37555 Einbeck, Germany (T.P.); Department of Agricultural Sciences, University of Bologna, 40127 Bologna, Italy (R.T.); MTA ATK/ AI CAR HAS, Martonvasar 2462, Hungary (Z.B.); UCL ELIA, 1348 Louvain-la-Neuve, Belgium (X.D.); and Institute for Botany and Molecular Genetics, BioSC, RWTH Aachen University, 52074 Aachen, Germany (B.U.)

ORCID IDs: 0000-0003-0758-9930 (S.D.N.); 0000-0002-2654-8125 (N.R.); 0000-0001-9143-9569 (R.T.); 0000-0001-9480-0532 (Z.B.); 0000-0002-3637-3330 (X.D.).

Assessing the genetic variability of plant performance under heat and drought scenarios can contribute to reduce the negative effects of climate change. We propose here an approach that consisted of (1) clustering time courses of environmental variables simulated by a crop model in current (35 years × 55 sites) and future conditions into six scenarios of temperature and water deficit as experienced by maize (*Zea mays* L.) plants; (2) performing 29 field experiments in contrasting conditions across Europe with 244 maize hybrids; (3) assigning individual experiments to scenarios based on environmental conditions as measured in each field experiment; frequencies of temperature scenarios in our experiments corresponded to future heat scenarios (+5°C); (4) analyzing the genetic variation of plant performance for each environmental scenario. Forty-eight quantitative trait loci (QTLs) of yield were identified by association genetics using a multi-environment multi-locus model. Eight and twelve QTLs were associated to tolerances to heat and drought stresses because they were specific to hot and dry scenarios, respectively, with low or even negative allelic effects in favorable scenarios. Twenty-four QTLs improved yield in favorable conditions but showed nonsignificant effects under stress; they were therefore associated with higher sensitivity. Our approach showed a pattern of QTL effects expressed as functions of environmental variables and scenarios, allowing us to suggest hypotheses for mechanisms and candidate genes underlying each QTL. It can be used for assessing the performance of genotypes and the contribution of genomic regions under current and future stress situations and to accelerate breeding for drought-prone environments.

With climate changes, crops will be subjected to more frequent episodes of drought and high temperature that may threaten food security (IPCC, 2014). Reducing the impacts of these effects is an urgent priority that (not exclusively) involves the genetic progress of plant performance under heat and drought stresses (Tester and Langridge, 2010; Lobell et al., 2011). Because hundreds of new genotypes of most cereals are commercialized every year, a generic approach is needed to avoid an endless series of experiments assessing the performances of the newly released genotypes. A systematic exploration of the natural genetic diversity used in breeding can provide information usable for large groups of genotypes. This entails the identification, among the thousands of accessions existing in gene banks, of allelic variants exhibiting specific adaptation traits by addressing three questions: (1) Is there a genetic variability for yield and related traits in dry and hot environments? (2) Can this genetic variability be dissected into the effect of genomic regions (quantitative trait loci, QTLs), and (3) have these genomic

[1] This work was supported by the European project FP7-244374 (DROPS) and the Agence Nationale de la Recherche project ANR-10-BTBR-01 (Amaizing).

* Address correspondence to francois.tardieu@supagro.inra.fr.

The author responsible for distribution of materials integral to the findings presented in this article in accordance with the policy described in the Instructions for Authors (www.plantphysiol.org) is: Francois Tardieu (francois.tardieu@supagro.inra.fr).

E.J.M., C.W., and F.T. designed the research and wrote the manuscript; E.J.M., C.W., F.T., W.K., F.v.E., A.C., A.C.-L., S.N., and S.D.N. analysed and interpreted data; E.J.M., C.W., S.N., S.D.N., X.D., and B.U. collected the data; S.P., N.R., T.P., R.T., and Z.B. coordinated fieldwork, performed experiments, and conducted primary data analysis; J.L., C.B., and C.W. generated the plant material.

[OPEN] Articles can be viewed without a subscription.

www.plantphysiol.org/cgi/doi/10.1104/pp.16.00621

regions differential effects depending on environmental conditions (QTL × environment interaction)? Advances in DNA marker analyses and sequencing technologies have decreased the cost of genotyping so the genome of thousands of plants can be densely characterized (Langridge and Fleury, 2011). Genome-wide association study (GWAS) allows associations of phenotypic traits with causal polymorphisms (Zhu et al., 2008) but, in our analysis, needs to be fine-tuned for plant responses to climatic scenarios associated with climate change. In particular, several options exist for the experimental strategy. (1) The comparison of genotype performances can be addressed in controlled infrastructures that simulate conditions in 2050—for instance, in phenotyping platforms (Tardieu and Tuberosa, 2010; Fiorani and Schurr, 2013) or in fields with managed environments (Salekdeh et al., 2009; Bishop et al., 2015). However, these possibilities do not address the diversity of environmental scenarios faced by plants in current and future conditions. (2) Panels of genotypes can be analyzed in a network of field experiments, resulting in the association of performances with genomic regions depending on environmental indices that best account for QTL×E interaction (Vargas et al., 2006; Malosetti et al., 2013; Bouffier et al., 2015). However, each network of experiments results in its own set of indices that cannot be easily compared between studies, nor extended to a whole geographic region.

We propose here an approach that consists in utilizing the current year-to-year and site-to-site climatic variability for genetic analyses of plant performance in current climatic scenarios and in those predicted for the future. It consists of (1) clustering current and future environmental conditions into a limited number of scenarios as experienced by the studied crop; (2) performing a series of field experiments for a collection of scenarios across Europe; (3) assigning individual experiments to scenarios according to environmental conditions measured in each field experiment; and (4) analyzing the genetic variation for plant performances as a function of environmental scenarios. Here, we address these four steps for maize (*Zea mays* L.) in Europe. Maize was chosen as a case study because it is a C_4 species in which the increase of CO_2 has limited effect on photosynthesis.

(1) The first step has been performed by running crop simulations over a large range of sites over tens of years and then clustering the simulated time courses of environmental variables into a limited number of environmental scenarios at key phenological stages of the crop (Chapman et al., 2000; Chenu et al., 2011). To address the case of maize grown in Europe, we have used the drought scenarios defined by Harrison et al., (2014) based on 55 European sites over 35 years. We have used the dataset collected in their paper to also identify three scenarios of temperature during the maize cropping cycle under current conditions. Future conditions have been simulated by using the model LARS-WG (Semenov and Stratonovitch, 2010).

(2) The second step consisted in performing field experiments with a panel of genotypes over a range of conditions. This was done in 29 field experiments (defined as combinations of site × year × watering regime), in which a panel of 244 maize hybrids was analyzed along a climatic transect from west to east Europe, plus one experiment in Chile. This panel, genotyped with 515 000 single nucleotide polymorphism (SNP) markers, maximized the genetic variability in the dent maize group while restricting the range of flowering time to 10 d in order to avoid confounding the effects of phenology with intrinsic responses to drought and heat. It included first-cycle lines derived from historical landraces and more recent lines created by public institutions and breeding companies.

(3) The third step ascribed each experiment to an environmental scenario defined in step 1. This required full environmental characterization of each individual experiment. We expected that the proportion of experiments belonging to each environmental scenario might appreciably differ from those calculated over 55 sites × 35 years. Hence, this step allowed us to give a weight to each experiment according to environmental conditions in this experiment and to frequencies of environmental scenarios. It was therefore not a simple classification of experiments of the network as performed by other groups (Vargas et al., 2006; Malosetti et al., 2013; Bouffier et al., 2015).

(4) The fourth step consisted in evaluating the genetic variability of yield and of related variables within each climatic scenario, in identifying genomic regions associated with these traits in each scenario and in relating allelic effects to measured environmental conditions. Indeed, associations between markers and yield under stress pose a specific challenge because every significant marker may have opposite allelic effects depending on the timing and severity of drought or heat stresses (Vargas et al., 2006; Boer et al., 2007; Collins et al., 2008; Tardieu, 2012). The analysis of a network of dry field experiments has shown that a given allele at a QTL can have a markedly positive effect in one category of experiments, a markedly negative effect in another category, and nearly no effect in half of experimental fields (Bonneau et al., 2013). Hence, we have first performed single-environment GWAS that allows identification of QTLs strongly associated with specific experiments and multi-environment GWAS that allows identification of QTLs with both main effect and QTL × E effects (Boer et al., 2007; Maccaferri et al., 2008; Malosetti et al., 2008a; Maccaferri et al., 2016). We have then analyzed the effects of QTL alleles conditional on scenarios and measured environmental conditions.

We could, in this way, estimate the frequencies of positive, negative, or null effects for each QTL in each climatic scenario, depending on measured environmental conditions in each field. This resulted in a pattern of QTL effects as a function of scenarios, environmental variables (e.g. temperature versus evaporative demand versus soil water potential) and traits

(e.g. flowering time versus grain number versus grain size). We have deduced from these patterns hypotheses for the mechanisms underlying the QTLs, thereby helping in the selection of candidate genes among the small number of possible genes close to causal polymorphisms. Hence, this work aimed to bring together GWAS and ecophysiological analyses for modeling and providing biological/ecological interpretation of conditional QTL effects associated to ranges of soil water deficit, evaporative demand, and air temperature across Europe in current and future climatic scenarios.

RESULTS

Environmental Scenarios in the Network of 29 Experiments Corresponded to Future Climatic Scenarios of Heat (+5°C) but Respected the Frequencies of Current Scenarios for Water Deficit

Temperatures had a large site-to-site variability (Fig. 1, A–G, Supplemental Table S1). Meristem temperature during the night (T_{night}) during 20 equivalent days at 20°C ($d_{20°C}$) around flowering time of the reference hybrid ranged from 15.6°C to 23.9°C, maximum meristem temperature (T_{max}) from 27.1°C to 37.9°C, and maximum vapor pressure difference between leaf and air (VPD_{max}) from 2.3 kPa to 4.2 kPa. These temperatures were considerably warmer than the means over the last 35 years in 55 European sites, referred to as "present" hereafter. The most frequent temperature scenario was *Hot* in which mean T_{night} and T_{max} were higher than 20°C and 33°C, respectively. It was observed in 14 experiments (Fig. 1C, 48% of cases versus 0.2% at present). The second was *Hot*(*day*), involving T_{max} above 33°C but T_{night} lower than 20°C, observed in eight experiments (Fig. 1D, 28% versus 0.8% at present). The *Cool* scenario with mean T_{night} and T_{max} lower than respective thresholds was observed in seven experiments (Fig. 1E, 24% versus 99% at present). Hence, the proportions of temperature scenarios in the network of experiments were broadly similar to those in a climatic scenario with a simulated increase in temperature of 5°C. This may be due either to a slight overrepresentation of southern sites in the network of experiments compared to the 55 European sites (mean latitude 45.8° versus 46.4°) or to warmer climatic years than average due to climate change. T_{max} and VPD_{max} were loosely related with incident light (r = 0.22 ns and 0.24 ns, respectively, Supplemental Table S2A; see also the principal component analysis in Supplemental Fig. S1, A and B).

Mean soil water potential (Ψ_{soil}) ranged from −0.01 to −0.42 MPa during 20 $d_{20°C}$ around flowering time of the reference hybrid, representing about 80% of the range of available water in most agricultural soils as estimated using the equations of Van Genuchten (1980). During this period, Ψ_{soil} was not correlated with T_{max} nor VPD_{max} (r = −0.13 ns and −0.34 ns; Supplemental Fig. S1, A and B). The four scenarios of soil water status identified by Harrison et al. (2014) were used for clustering experiments. These scenarios were originally based on the supply/demand ratio for water as simulated by the APSIM model. Here, they were expressed based on soil water potential measured at three soil depths every day, in such a way that scenarios based on supply/demand and on soil water potential matched in those fields in which we had sufficient data to carry out both approaches. The first scenario (*WW cycle*),

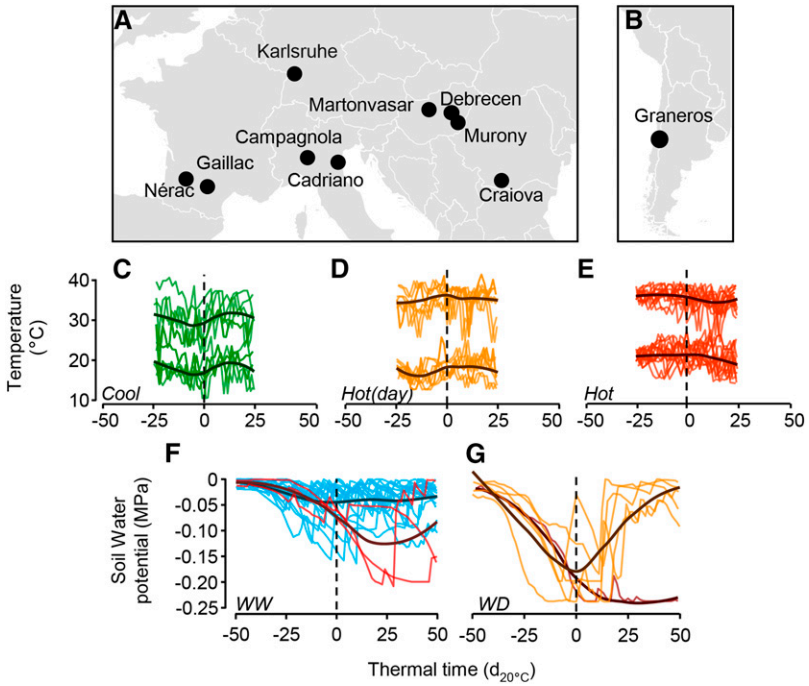

Figure 1. Time courses of soil water potential and temperature in each environmental scenario. A and B, Each line represents a time course corresponding to one experiment of the field network in Europe (A)or Chile (B). C to G, time courses were centered (time 0) on the day of anthesis of the reference hybrid (vertical dashed line). Dark lines represent smoothed mean values. Thermal time is in equivalent days at 20°C. C, experiments with cool temperatures during both day and night (*Cool*); D, experiments with hot temperatures during the day but cool temperatures during the night (*Hot*(*day*)); E, experiments with hot temperatures (*Hot*, mean maximum temperatures > 33°C and mean night temperatures > 20°C). C to E, The upper series of lines represents maximum temperature and the lower series represents mean night temperature. F, Well-watered experiments (*WW*) with experiments in which mean soil water potential was higher than −0.10 MPa (*WW cycle*, blue lines) and experiments with well-watered conditions during flowering time and water deficit during grain filling (*late Term*, red); G, Water deficit experiments (*WD*) with early deficit followed by recovery at flowering time (*Rec*, yellow lines) and experiments with water deficit from vegetative stage to maturity (*early Term*, dark red lines).

involving favorable soil water status throughout the crop season, was observed in 18 experiments (62% of cases if a threshold of Ψ_{soil} was set at −0.1 MPa; Fig. 1F; Supplemental Table S1) versus 41% of maize fields over Europe in current conditions (Harrison et al. 2014). Most *WW cycle* experiments showed average Ψ_{soil} between −0.01 and −0.04 MPa except two. The second most frequent scenario involved water deficit during flowering time followed by recovery (*Rec*) and was observed in five experiments (17%) versus 18% of scenarios over Europe in Harrison's study (Fig. 1G; Supplemental Table S1). The last two scenarios with early or late terminal stresses (*early* and *late Term*, respectively) were less frequent (seven experiments, 24%) than over Europe (40% in Harrison's study; Fig. 1, F and G; Supplemental Table S1). The resulting number of combined water × temperature scenarios was too large in relation to the number of experiments, so scenarios of soil water status were grouped in two classes (WW and WD, Figure 1, F and G). Because grain number is determined 10 d after anthesis (Oury et al., 2016a, 2016b), we have grouped, on the one hand, scenarios *WW cycle* and *late Term* (Fig. 1F) with favorable Ψ_{soil} at flowering time and, on the other hand, *Rec* and *early Term* (Fig. 1G) with water deficit at flowering time. For grain size, the scenarios were grouped depending on the water status during grain filling (*WW cycle* and *Rec* with high water potential versus both *Term* scenarios of water deficit). The scenarios for yield followed those for grain number in view of the high correlation between both traits (Fig. 2A; Supplemental Table S1).

Overall, experiments were therefore clustered in six scenarios obtained by the combination of two water scenarios and three temperature scenarios. Incident light cumulated during the same phenological stage ranged, in European sites, from 256 to 594 MJ m^{-2} (Supplemental Table S1) and were higher in the Chilean experiment (682 and 776 MJ m^{-2}). It did not significantly differ between scenarios, from 379 to 487 MJ m^{-2}, except for the scenario that included the Chilean experiments. Day length at floral transition of the reference hybrid ranged from 15.3 to 16.0 h in European sites and was 14.2 h in the Chilean experiment (Supplemental Table S1).

Variations of Mean Yield between Experiments Depended on Temperature, Evaporative Demand, and Soil Water Status around Flowering Time

Grain yield averaged over the whole panel ranged from 1.5 to 11.2 t ha^{-1} in our experiments (from 1.2 to 12.9 t ha^{-1} for best linear unbiased estimators (BLUEs) of the reference hybrid; Fig. 2A; Supplemental Table S1). The respective differences in yield between sites and within each site is illustrated in Figure 3, A, C, and E, for three experiments in either favorable conditions or with water deficit or high temperature. Large differences in yield were observed between experiments in each scenario but with an overlap between the distributions of yields in the panel (Supplemental Fig. S2). Figure 4 presents the genotypic variability of yield for hybrids belonging to the first (Fig. 4, A–C) and third (Fig. 4, D–E) quartile of yield values in *WW-Cool* scenarios, ordered in each quartile by yield values in the scenario *WW-Hot* (all hybrids are presented in Supplemental Fig. S3 and Supplemental Table S3). Highest yields and grain numbers were observed in experiments classified as *Cool-WW* (10.8 t ha^{-1} average for the reference hybrid, 9.4 t ha^{-1} for panel mean; Fig. 4; Fig. 2A, blue ellipse) while experiments in WD-*Hot* had the lowest yields (4.6 and 4.5 t ha^{-1}). Within *WW* experiments, yield was much lower in *Hot* than in *Cool* scenarios, with a smaller effect in *Hot*(*day*) scenarios (Fig. 4). This pattern applied to hybrids with yield either in the first or the fourth quartile. It is noteworthy that the classical distinction between rain-fed and irrigated fields did not help in this analysis. Indeed, coefficients of variations of yield were 52% and 35%, respectively,

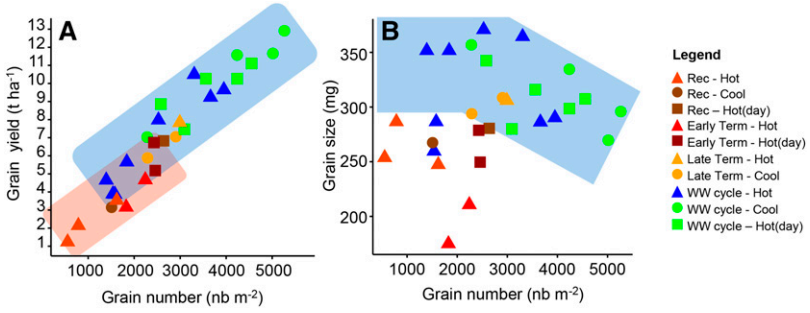

Figure 2. Relationship between grain yield and grain number (A) and between grain size and grain number (B) for the reference hybrid. Each symbol corresponds to one experiment. Blue and green symbols, Well-watered experiments (*WW cycle*); brown, experiments with early deficit followed by recovery (*Rec*) at flowering time; red, experiments with water deficit from vegetative stage to maturity (*early Term*); orange, experiments with water deficit during grain filling (*late Term*). Symbol shape indicates temperature at flowering time. Circle, Cool temperatures; triangles, hot temperatures; squares, temperatures cool during the night but hot during the day. Blue shapes in A and B indicate the region of the panel with maximum density of well-watered experiments during grain filling (*WW cycle* and *Rec*). Salmon shape indicates experiments with water deficit during grain filling (*Term*).

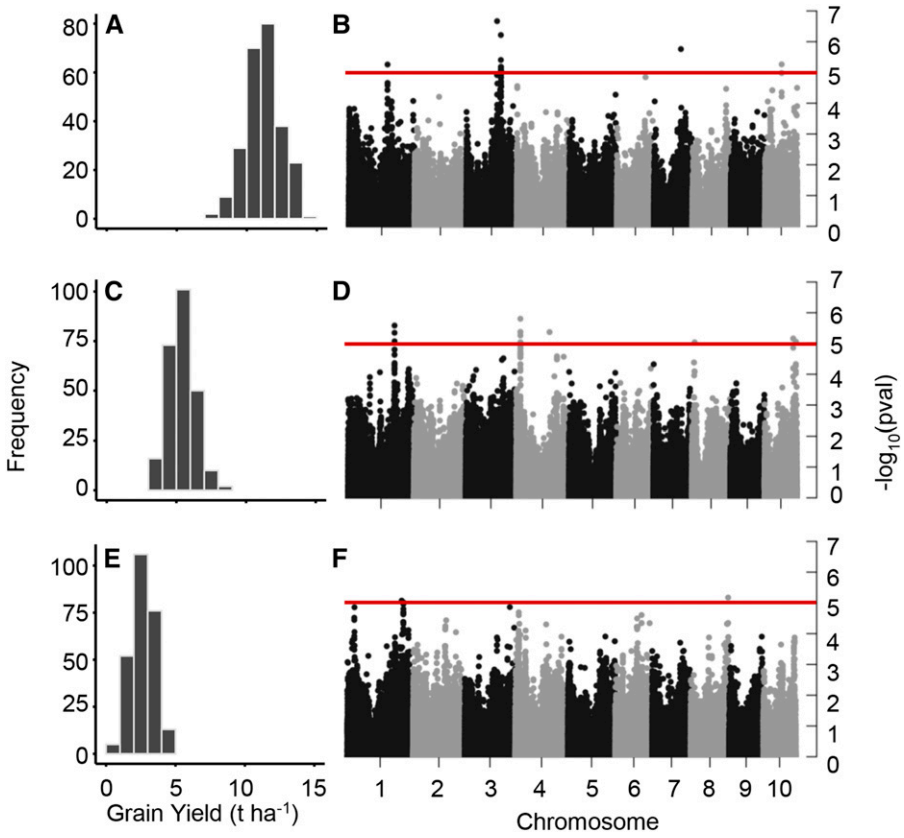

Figure 3. Genetic variability of grain yield in three typical experiments. A and B, Well-watered soil and cool air temperature at flowering time (Gai12W); C and D, well-watered soil and hot air temperature at flowering time (Cam13W); E and F, soil water deficit plus hot air temperature (Bol12R). Histograms are based on the BLUEs values of grain yield (A, C, and E) estimated with a mixed model (Supplemental Methods S1). Manhattan plots show results of single-environment GWAS (B, D, and F), with the red line indicating the -$\log_{10}$(*P* value) threshold of 5.

in irrigated and rain-fed regimes (means, 8.3 and 5.9 t ha^{-1} for the reference hybrid), consistent with the fact that Ψ_{soil} at flowering time largely varied within watering regimes. Because of high rainfall, four rain-fed fields were WW (Ψ_{soil} higher than −0.01 MPa; Supplemental Table S1), whereas one irrigated field was in water deficit (Ψ_{soil} down to −0.42 MPa) because of restrictions of irrigation (Supplemental Table S1).

Overall, environmental variables that best accounted for yield were T_{night} and Ψ_{soil} at flowering time (r = -0.56 *P*-value < 0.01 and 0.50 *P*-value < 0.01 respectively, for the reference hybrid, Supplemental Table S2B). The

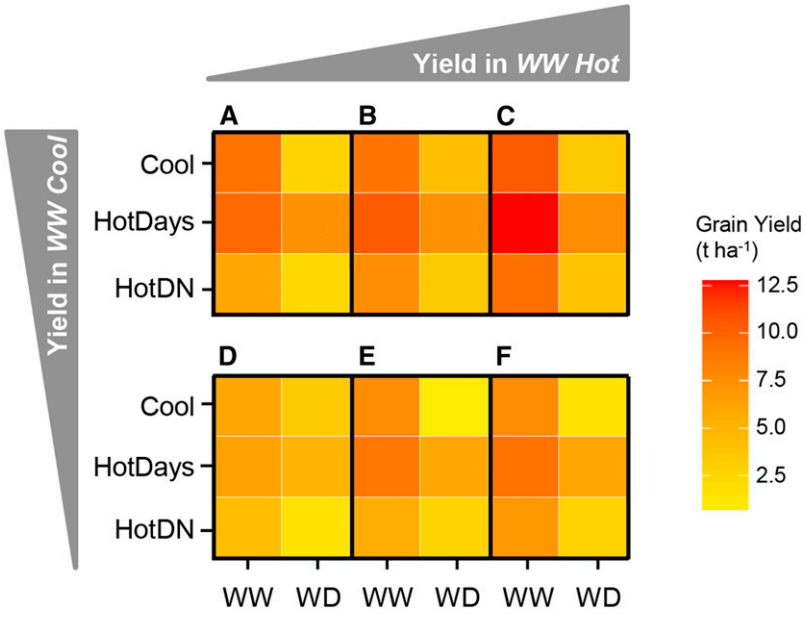

Figure 4. Genetic variability of grain yield in the six studied environmental scenarios. Variability of grain yield for six hybrids in the environmental scenarios identified in Fig. 1 (*WW cycle* and *lateTerm* are grouped as WW, *Rec*, and *early Term* are grouped as WD, see text). A to C, Hybrids with high performance in *WW-Cool* (first quartile of yield), D to F, hybrids with lower performance in *WW-Cool* (third quartile of yield). Three hybrids are shown in each category, classified by yield values in the scenario *WW-HotDN*, ranked as first, median, and last for yield in each quartile. Accessions of genotypes are as follows: A, PHG47_usda; B, B84_inra; C, Lo1087_bergamo; D, Pa36_inra; E, F7058_inra; F, Mo15W_inra.

same correlations were significant for all hybrids (P value < 0.01) with values ranging from -0.59 to -0.52 for T_{night} and from 0.42 to 0.49 for Ψ_{soil}. The amount of light cumulated either for the whole cycle or during flowering time had no clear relation with yield or grain number (r = 0.11 ns and 0.01 ns, respectively). Differences in yield between experiments were essentially accounted for by grain number per unit area in WW scenarios at flowering time (*WW cycle* and *Rec*; Fig. 2A). This suggests a major effect of environmental conditions during the vegetative and flowering phases. Grain size was high in these scenarios, with a loose, negative relation with grain number indicating a source limitation at high grain numbers (r = -0.27 in the reference hybrid, Figure 2B). Most experiments with terminal water deficit (*early* and *late Term*) had a lower grain size at a given grain number (Fig. 2B). Yield was still related to grain number in these scenarios but at lower values due to a lower individual grain size (P value < 0.05 for differences in intercepts). The relationships corresponding to other hybrids shared most of the features presented in Figure 2 (Supplemental Fig. S4, A and B). Grain number was positively related to Ψ_{soil} and negatively to T_{night} and T_{max} (r = 0.37; P value < 0.1, -0.54 P-value < 0.01, and -0.44 P value < 0.05, respectively; correlations were significant for the reference hybrid and for 94% of hybrids, Supplemental Table S2C). Grain size was positively related to Ψ_{soil} and negatively to T_{night} during grain filling (r = -0.38; P value < 0.05 and 0.67 P value $<$ 0.001, respectively, Supplemental Table S2D). Maximum *VPD* and T_{max} had slightly lower overall effects on grain yield (r = -0.22 ns and -0.36 ns, respectively, ranging from -0.35 to -0.25 and from -0.18 to -0.07).

High Genetic Variability and G×E Interaction for Yield and Yield Components

The panel showed a large genetic variability of yield and yield components within each experiment, with a genotypic variation (G) affecting mean yield by ± 18% (Table I), and a genetic coefficient of variation ranging from 0.10 to 0.49 (0.08 to 0.42 for grain number and 0.03 to 0.11 for grain size; Supplemental Table S4A). This variability applied within each environmental scenario (Fig. 4): Yield in the scenario *WW-Hot* ranged from 5.8 to 9.1 t ha^{-1} in highest yielding hybrids (first quartile of yield; Fig. 4, A–C). The difference in yield between *WW-cool* and *WW-Hot* ranged from 3.1 t ha^{-1} (sensitive hybrids) to 1.2 t ha^{-1} (stable hybrids). The same pattern applied to hybrids in the third quartile (Fig. 4, D–F). This illustrates the genotype × scenario interaction (G × EC), which affected the yield mean by ± 6% (Table I) and captured part of the interactions with location (G × L, ± 10%), year (G × Y, ± 7%), and location by year (G × Y × L, ± 11%; Table I). The same analysis gave similar results for grain number, while both G and G × E were lower for grain size (Supplemental Table S5, A and B). Narrow sense heritabilities for grain yield ranged from 0.19 to 0.84 with a median of 0.52 (Supplemental Table S4A). Slightly smaller heritabilities were observed for grain number and grain size (Supplemental Table S4, B and C). Experiments in the *WW* group showed more heritable grain yield than in *WD* group (h^2 = 0.56 and 0.37, respectively). Within the *WW* group, heritabilities were independent of temperature (h^2 = 0.54 in *Cool*, 0.53 in *Hot*(*day*), and 0.58 in *Hot*).

The genotypic variation of time to anthesis was from 63.9 to 75.9 $d_{20°C}$ in the panel, with narrow sense heritabilities from 0.19 to 0.83 (median = 0.68). The correlation between time to anthesis and yield tended to be positive in *WW* fields (r from 0.10 ns to 0.56, P value $<$ 0.001; data not shown), indicating that latest hybrids had slightly higher yield and grain number than earlier hybrids, most likely due to a longer cumulated photosynthesis. This correlation was not observed in fields with terminal water deficit, and was even negative in fields in which plants experienced most severe terminal stress, typical of an avoidance strategy (e.g. r = -0.38, P value < 0.001 in Bol12R).

Genomic Regions Controlling Grain Yield Displayed Scenario-Dependent Effects

The single environment (SE) and multi-environment (ME) GWAS together identified 467 SNPs significantly associated with grain yield, as illustrated in Figure 3 for three experiments, 296 with grain number and 215 with grain size. Significant SNPs were then grouped according to genetic distances, with a threshold at 0.1 cM, leading to the identification of 115 QTLs for grain yield,

Table I. *Variance components of the different mixed models for grain yield*

Statistical Model	Type	G[a]	G × EC[b]	G × L[c]	G × Y[d]	G × L × Y[e]	Res[f]
Model M1: Multi-envt	Variance component (t ha^{-1})^2	0.359		0.130	0.054	0.133	0.480
Model M2: Multi-envt + EC	Variance component (t ha^{-1})^2	0.353	0.039	0.118	0.053	0.140	0.452
Model M3: Multi-envt, multilocus	Variance component (t ha^{-1})^2	0.074	0.012	0.064	0.039	0.080	0.370
Model M1: Multi-envt	SD as % of mean	9.1		5.5	3.5	5.5	10.5
Model M2: Multi-envt + EC	SD as % of mean	9.0	3.0	5.2	3.5	5.7	10.2
Model M3: Multi-envt, multilocus	SD as % of mean	4.1	1.7	3.9	3.0	4.3	9.3
QTLs (diff. var. comp. model 2–3 in %)		79	69	45	26	43	18

The general mean of grain yield was 6.57 t ha^{-1}. [a]Genotype. [b]Genotype by environmental classification. [c]Genotype by location. [d]Genotype by year. [e]Genotype by location by year. [f]Experiment-specific residual error variances.

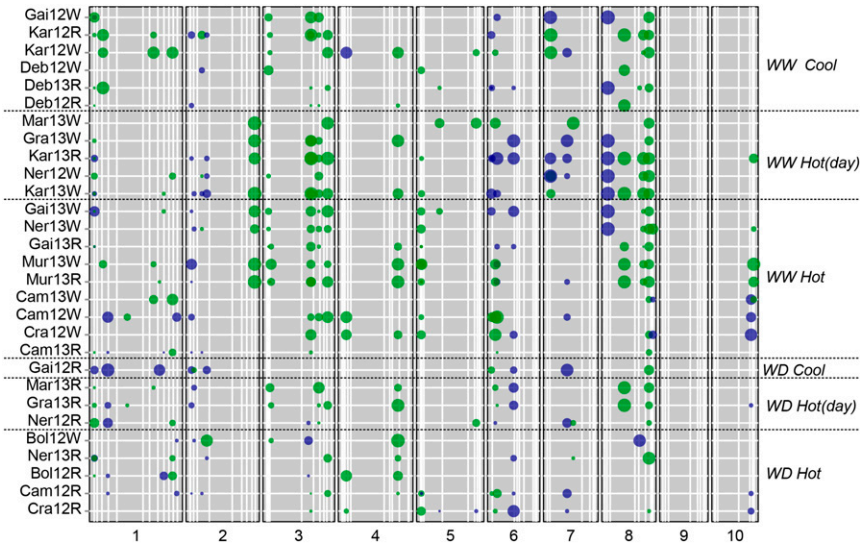

Figure 5. Final set of significant QTLs for grain yield in the 29 experiments. Circle diameters are proportional to the absolute value of allelic effect. Colors indicate the direction of effect: green when the reference hybrid allele increases grain yield, and blue when the other allele increases grain yield. Physical positions of the markers are based on the B73 reference genome RefGen_v2. Each horizontal line contains QTLs of one experiment, organized by scenarios of water status and temperature. Vertical white lines indicate bin position (bins are subdivisions of chromosomes in maize).

84 QTLs for grain number, and 105 QTLs for grain size. The number of QTLs for grain yield was reduced to 48 after backward elimination (Fig. 5; Table II). These QTLs captured 79% of the additive genetic variance (Table I) and large part of the G × E, in particular 69% of the interaction between genotype and environmental scenarios (G × EC). Individually, six QTLs retained 10% or more of the genetic variance, and five QTLs captured more than 10% of the G × EC (data not shown). The 48 QTLs appeared on average in seven experiments, from 2 to 23 (Fig. 5; Supplemental Table S5). Forty-six QTLs were identified for grain number and 33 for grain size after backward elimination (Supplemental Fig. S5, A and B).

Among the resulting 48 QTLs of grain yield, 38 displayed significant interaction with environmental scenarios (27 QTLs for grain number and 23 QTLs for grain size, Supplemental Table S6; Supplemental Table S7, A–D). This is illustrated in Figure 6, in which the allelic effects of 12 QTLs are presented in each scenario (see Supplemental Figure S6 for heat maps of the remaining 36 QTLs). The interaction between QTL and scenario (QTL × EC) can be visualized by the fact that allelic effects of a given QTL ranged from negative to highly positive depending on scenarios, with patterns analyzed hereafter. Fourteen interactions were significant for water scenarios and 18 for temperature scenarios, including 11 QTLs significant for both water and temperature scenarios. Temperature scenarios were tested in WW only to avoid confounding effects.

Combining the Analyses QTL × Scenarios and QTL × Environmental Variable Increased Insight and Allowed Identification of QTLs Associated to Tolerance to Water Deficit and High Temperature

The 48 QTLs of yield were classified in groups defined by the conditional effect of their alleles (Fig. 5; Table II; Supplemental Table S6) based on discrete environmental scenarios as above, combined with a continuous analysis with individual environmental variables (Fig. 7).

Eight QTLs Showed Significant Responses to Temperature with Large Allelic Effects at High Temperatures and Small or No Effects in Cool Temperature/Low Evaporative Demand

These QTLs can be qualified as providers of heat tolerance because their allelic effects ranged from slightly negative in cool situations (−0.16 to −0.05 t ha^{-1}) to highly positive in hot situations (+0.22 to +0.47 t ha^{-1}; Fig. 5; Table II). They harbored from two to 16 genes, except the QTL on bin 6.01 (Table II). Some of them are presented with more detail below.

A QTL on bin 6.01 (18.9 Mb, Fig. 6A) had a largely positive effect (+0.36 t ha^{-1}) in *Hot* scenarios, was significant in most *Hot*(*day*) scenarios (Fig. 5) and had lower effects in other scenarios (even reversed in *WD-Cool* scenarios). The environmental variable best related to QTL effect was VPD_{max}, with maximum effect at VPD_{max} higher than 3 kPa versus negligible effects at low VPD_{max} or T_{max} (Fig. 7A). It affected yield and grain number, but not grain size, suggesting that it acted during the vegetative period or flowering time. Because allelic effects were significantly related to VPD_{max} (r = 0.32), but not to T_{night} (r = -0.05), it is likely to act via transpiration rate. A candidate gene was identified in the QTL region (Supplemental Table S7), whose effect is consistent with the above analysis. It codes for an ABA/water deficit stress induced protein (Canel et al., 1995; Padmanabhan et al., 1997). Three QTLs of this category on bins 6.01 (25.6 Mb), 10.06 (141.6 Mb), and 5.01 (5.8 Mb) are illustrated in Figure 6, B to D. Three genes involved in ABA or ethylene responses were identified in the region of the QTL on bin 10.05 (132.2 Mb, Supplemental Table S7).

Table II. *Final set of QTLs for grain yield (t ha^{-1}) with position, effects, scenarios with minimum and maximum effects and number of genes in the region around QTL position*

SNP Name[a]	SNP position (pb)[b]	Chr[c]	Bin[c]	Region (Mbp)[d]	Region (cM)[d]	-log$_{10}$(*P*)	Allelic effect range (t ha^{-1})		Scenarios with min. effects[f]	Scenarios with max. effects[g]	Nb of genes[h]
							Min[e]	Max[e]			
QTLs of Tolerance to High Temperature or Evaporative Demand											
AX-90681970	119501405	1	1.05	118.51–120.62	113.97–114.17	5.3	−0.12	0.22	All Cool	All Hot	16
AX-90728209	295726849	1	1.11	295.51–295.79	256.97–257.48	5.9	−0.13	0.25	WD Cool	WD Hot	10
AX-91388323	17398949	3	3.04	17.29–17.52	49.9–50.1	5.1	−0.10	0.31	WW Cool	WW Hot	3
AX-91419621	5773880	5	5.01	5.74–5.81	20.61–20.81	5.5	−0.09	0.29	WD Cool	All Hot	7
AX-90548584	18990406	6	6.01	11.12–24.47	9.34–9.56	13.4	−0.16	0.36	WD Cool	WW Hot	153
AX-91685911	25582930	6	6.01	24.88–25.9	9.64–9.92	5.4	−0.11	0.44	WW Cool	All Hot	6
AX-90648418	132186162	10	10.05	132.09–132.35	84.93–85.21	6.2	−0.05	0.38	WW Cool	WW Hot	11
AX-91194279	141619465	10	10.06	141.6–141.65	109.54–109.74	5.2	−0.10	0.47	WD Cool	WW Hot	2
QTLs of Tolerance to Water Deficit or to Combined Water Deficit and High Temperature											
AX-90663757	50439360	1	1.03	50.21–51.01	71.48–71.82	6.1	−0.07	0.44	WW Cool	WD Cool	9
AX-90711265	234219088	1	1.08	234.14–234.31	193.55–193.75	5.0	−0.15	0.32	WW Cool	WD Cool	7
AX-91499584	249530930	1	1.08	249.35–249.72	205.47–205.67	5.1	−0.17	0.24	WW Hot(day)	WD Cool	14
AX-90636164	280572987	1	1.10	280.5–280.66	230.44–230.66	5.4	−0.16	0.34	WW Hot(day)	WD Cool	10
AX-90734735*	16773313	2	2.03	16.73–16.82	54.4–54.6	5.1	−0.19	0.19	WW Hot(day)	WD Cool	1
AX-91517386*	44474968	2	2.04	44.29–44.67	81.95–82.16	5.7	−0.20	0.24	WW Cool	WD Cool	13
AX-90832809	150434035	3	3.05	150.2–150.8	65.67–65.93	5.4	−0.16	0.25	All WW	All WD	4
AX-90629633*	16418312	4	4.03	16.36–16.5	38.31–38.51	5.0	−0.34	0.34	WW Hot(day)	WD Hot	3
AX-90648211	200188443	4	4.08	199.03–201.47	114.21–114.41	5.2	−0.05	0.55	WW Cool	WD Hot	50
AX-90979819*	6613959	6	6.00	6.52–7.28	6.88–7.6	9.3	−0.23	0.26	WW Cool	WD Hot	21
AX-90998525	84384458	6	6.01	84.28–84.49	16.99–17.19	5.9	−0.02	0.43	WW Cool	All WD	3
AX-91101271	125931027	8	8.05	125.87–125.99	110.13–110.39	5.4	−0.18	0.36	WW Cool	WD Hot	2
QTLs of Plant Performances that Disappeared under Stressing Conditions											
QTLs Associated with a Comparative Advantage in WW											
AX-90650418	2797566	1	1.01	2.76–2.85	6.07–6.27	5.2	−0.11	0.29	WD Hot(day)	WW Hot(day)	5
AX-90590040**	158974646	3	3.05	158.62–159.08	71.86–72.34	6.2	−0.02	0.34	All WD	All WW	5
AX-91642932	5435055	5	5.01	5.41–5.48	19.53–19.73	5.4	−0.10	0.25	All WD	All WW	3
AX-91366227	5155708	6	6.00	5.08–5.25	5.24–5.44	6.0	−0.22	0.29	WD Cool	WW Cool	3
AX-91685880	25317825	6	6.01	24.92–26.04	9.65–9.97	6.5	−0.15	0.38	WD Hot(day)	WW Hot(day)	6
AX-91072197	12782249	8	8.02	12.74–12.83	33.58–33.78	5.9	−0.25	1.34	All WD	All WW	3
AX-91105090	139338906	8	8.05	139.05–139.64	124.98–125.18	5.1	−0.05	0.39	All WD	All WW	9
QTLs Associated with a Comparative Advantage in Cool and Hot(day)											
AX-91203024	2430515	1	1.01	2.39–2.48	5.25–5.45	6.4	0.02	0.29	All Hot	All others	3
AX-90658944	33122606	1	1.03	32.96–33.29	63.8–64	5.6	−0.11	0.40	WW Hot(day)	WW Cool	6
AX-91510619	7524873	2	2.02	7.5–7.55	26.28–26.48	5.3	−0.06	0.31	WD Hot	WD Cool	2
AX-91520713	62023101	2	2.04	61.77–62.29	89.88–90.08	5.7	−0.24	0.34	WD Hot	WD Cool	6
AX-90973370	201266231	5	5.06	201.23–201.32	139.7–139.9	6.1	−0.16	0.31	All Hot	All Cool + Hot(day)	2
AX-91726785	75172928	7	7.02	55.33–81.98	38.92–39.12	5.4	−0.15	0.38	All Hot	All Cool + Hot(day)	166
AX-91201897	71654502	8	8.03	71.06–72.32	67.02–67.22	5.4	−0.10	0.60	WD Hot	All Hot(day)	16
QTLs Associated with a Comparative Advantage in WW and Cool Conditions Only											
AX-91440967	212986628	1	1.07	212.87–213.18	163.66–164.02	5.6	−0.15	0.35	WD Hot	WW Cool	10
AX-90792361	232389200	2	2.09	232.35–232.46	201.29–201.53	5.5	−0.23	0.63	WD Hot	WW Cool + Hot(day)	8
AX-90796025	8267933	3	3.02	8.25–8.3	31.08–31.28	5.7	−0.08	0.27	WD Cool	WW Hot(day)	4
AX-91445849	13278110	3	3.04	13.23–13.34	44.38–44.58	5.8	−0.16	0.25	WD Hot	WW Cool	4

(*Table continues on following page.*)

Table II. (*Continued from previous page.*)

SNP Name[a]	SNP position (pb)[b]	Chr[c]	Bin[c]	Region (Mbp)[d]	Region (cM)[d]	-log$_{10}$(*P*)	Allelic effect range (t ha^{-1})		Scenarios with min. effects[f]	Scenarios with max. effects[g]	Nb of genes[h]
							Min[e]	Max[e]			
AX-90539808	187430601	3	3.06	187.3–187.53	117.84–118.08	5.3	0.02	0.33	WD Hot	All Hot(day)	10
AX-90597453	159743301	3	3.05	159.43–159.84	72.71–73.15	7.5	−0.12	0.56	WD Hot	WW Hot(day)	12
PZE-103171561	218787839	3	3.09	218.74–218.85	161.22–161.42	5.4	−0.05	0.49	All WD	WW Hot(day)	9
AX-91643166	6672502	5	5.01	6.64–6.71	23.42–23.62	5.2	−0.14	0.32	WD Hot	WW Hot(day)	4
AX-91654943	70841813	5	5.03	70.61–71.08	72.45–72.65	5.8	−0.14	0.27	WD Hot	WW Hot(day)	23
AX-91715582	15743645	7	7.02	15.55–15.95	34.22–34.42	5.3	−0.18	0.53	WD Hot(day)	WW Cool	3
AX-91026565	16948400	7	7.02	16.71–17.21	34.76–34.96	5.4	−0.18	0.53	WD Hot(day)	WW Cool	4
QTLs with No Clear Pattern of Allelic Effects											
AX-91405380**	159499687	8	8.06	159.43–159.58	136.69–136.89	6.4	0.03	0.39	High positive effect in all scenarios		4
AX-91047031	97064114	7	7.02	96.12–97.71	40.54–40.77	5.2	−0.14	0.41	No contrast for scenarios and no		11
AX-90571454	173077597	8	8.08	173.04–173.12	173.26–173.5	5.0	−0.24	0.31	relationship with any variable		8

*, QTLs that displayed inversion of effects; **, QTLs that colocated with QTLs of anthesis. [a]SNP with the highest –log$_{10}$(*P*-value). [b]SNP physical position. [c]Chromosome and bin (a subdivision of the maize chromosomes). [d]QTL region (in physical and genetic units). [e]Minimum and maximum effects in individual experiments. [f]Environmental scenarios in which allelic effects were minimum. [g]Environmental scenarios in which allelic effects were maximum. [h]Number of genes in the region of the QTL.

Twelve QTLs Showed Large Allelic Effects at Low Water Potentials and Small or No Effects in Moist Soils, in Combination or Not with Temperature Effects

These QTLs can be qualified as providers of drought tolerance. In eight of them, allelic effects ranged from slightly negative in WW situations (−0.02 to −0.18 t ha^{-1}) to highly positive in WD situations (+0.24 to +0.55 t ha^{-1}; Fig. 5; Table II). Four of these QTLs (bins 2.03, 2.04, 4.03, and 6.00) even showed clear inversion of effects in WW and WD scenarios, with −0.34 to −0.19 t ha^{-1} in WW and from +0.19 to +0.34 t ha^{-1} in WD scenarios. These QTLs harbored from one to 50 genes (median = seven genes).

For example, a QTL on bin 2.04 (44.5 Mb) showed inversion of allelic effects in WW and WD scenarios (Fig. 6H). It was found to constitutively affect leaf ABA content (Giuliani et al., 2005), consistent with the fact that a gene coding for a zeaxanthin epoxidase involved in ABA biosynthesis was identified in the region of the QTL (Supplemental Table S7). This could explain the inversion of allelic effects of this QTL in WW and WD scenarios because high ABA can cause reduction in growth in WW while maintaining growth in WD (Tardieu et al., 2010; Tardieu, 2012). Two QTLs on bins 3.05 (150.4 Mb) and 1.03 (50.4 Mb) had positive effects in WD scenarios but no significant effect in WW scenarios (Fig. 5; Fig. 6, E and F; Table II). Across scenarios, their allelic effects increased in dry soils (r = 0.63 and 0.43 with soil water potential, respectively; Fig. 7B), but also with evaporative demand (r = 0.51 and 0.48). The QTL on bin 3.05 colocated with a gene coding for a Cys-rich TM (Supplemental Table S7) with roles in stress response or stress tolerance (Venancio and Aravind, 2010) and a strong up-regulation under drought stress (Zheng et al., 2010). A QTL on bin 6.01 (84.4 Mb) showed similar pattern of allelic effects although with less effect of climatic scenarios (Fig. 6G). As the effects of the former two QTLs, it also correlated with evapotranspiration (r = 0.36) and VPD_{max} (r = 0.41). It colocated with a gene that codes for a protein of type zinc finger domain and may be involved in protein-protein interactions (K and Laxmi, 2014).

Two QTLs of Yield Acted via Changes in Flowering Time

The QTL on bin 3.05 (159.0 Mb; Fig. 6I) colocated with a QTL of flowering time in our dataset, as observed by another group (Salvi et al., 2011). It delayed flowering time by 0.8 $d_{20°C}$, and had a positive effect on yield in *WW* scenarios (16 experiments out of 20; Fig. 5), but not in *WD* scenarios, consistent with a correlation with Ψ_{soil} in which the QTL effect disappeared at −0.35 MPa (r = 0.63; Fig. 7C). The scenario-dependent effect on yield of this QTL is probably linked to the fact that it increased cumulated photosynthesis in well-watered conditions, while this effect disappeared under water deficit because of a negative impact of a late flowering time on soil water balance. Among the genes under this QTL, we have identified a gene coding for a

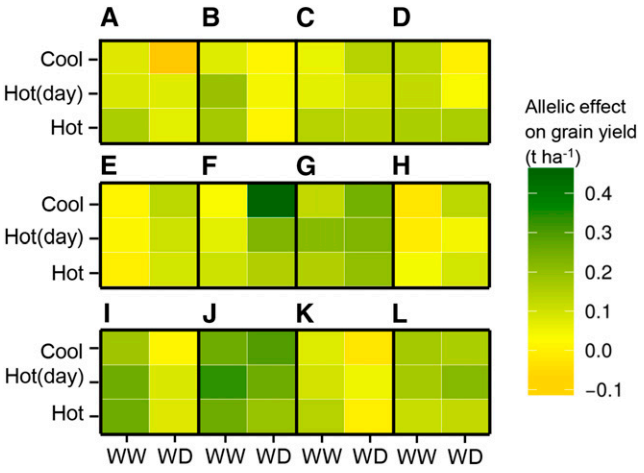

Figure 6. Heat map of the allelic effects of 12 QTLs of grain yield in the six environmental scenarios. Green, The allele increases grain yield; orange, the allele decreases grain yield; yellow, the effect is null. By convention, the plus allele is the one that is favorable for mean performance. Allelic effects were estimated per experiment and then averaged across experiments per environmental scenario. A to D, QTLs conferring tolerance to heat with high effect in *HotN* and null effect in *Cool*: A, bin 6.01 (18.9 Mb); B, bin 6.01 (25.6 Mb); C, bin 10.06 (141.6 Mb); D, bin 5.01 (5.8 Mb). E to H, QTLs conferring tolerance to drought with effects in WD and lesser or reversed effect in WW: E, bin 3.05 (150.4 Mb); E, bin 1.03 (50.4 Mb); G, bin 6.01 (84.4 Mb); H, bin 2.04 (44.5 Mb). I to L, QTLs of plant performance under favorable conditions with lesser effect in dry and hot conditions, including two genes affecting flowering time (I,K): I, bin 3.05 (159.0 Mb); J, bin 8.06 (159.5 Mb); K, bin 5.01 (5.4 Mb); L, bin 1.01 (2.4 Mb).

MADS box, which is a transcription factor class often involved in vegetative and reproductive developments (Supplemental Table S7). A common QTL for both yield and flowering time was also observed on bin 8.06 (159.5 Mb) in 23 experiments (Figs. 5 and 6J) with most often a highly positive allelic effect. Because this QTL shows smaller differential effects on yield in water and temperature scenarios (Table II) compared to that on bin 3.05, it may affect yield via another mechanism in addition to flowering time. It is noteworthy that this QTL is located at more than 15 cM from *vgt1*, a classical QTL of flowering time (Salvi et al., 2007).

Twenty-Five QTLs of High Plant Performance Disappeared under Hot or Dry Conditions

These QTLs were significantly associated with a comparative advantage in *WW* and/or cool conditions (from 0.25 to 1.34 t ha^{-1}), but their allelic effect decreased, disappeared, or even reversed under soil water deficit or high temperature (from −0.25 to +0.03 t ha^{-1}; Table II; Fig. 5). They are classified in Table II according to the environmental condition that had the larger detrimental effect on yield. They harbored from two to 23 genes (median = five genes), except one QTL that harbored 166 genes.

For example, a QTL on bin 5.01 (5.4 Mb; Fig. 6K) showed a larger allelic effect on yield in WW compared to WD scenarios. Seven QTLs were significant for grain yield in cool temperatures but disappeared at high temperature (Table II; Fig. 5) as shown in Figure 6L and Figure 7D for a QTL of grain yield on bin 1.01 (2.4 Mb) with a high correlation between its allelic effect and T_{night} (r = −0.42) and with T_{max} (r = −0.34). Eleven QTLs appeared only in WW and cool experiments and tended to disappear in hot and/or drought scenarios. This is consistent with candidate genes potentially involved in growth per se, such as a gene coding for a cell wall protein that affects cell wall mechanical properties (QTL on Bin 7.02, 75.2 Mb; Basu et al., 2016), with a cyclin-dependent protein kinase regulator (QTL on bin 3.06, 187.4 Mb) or in auxin signaling (QTLs on bins 3.04, 13.3 Mb, and 3.09, 218.8 Mb; Supplemental Table S7).

Three QTLs Did Not Display a Clear Pattern of Allelic Effect in Environmental Scenarios

We have classified in this category the QTL on bin 8.06 (159.5 Mb) presented above because it had a positive allelic effect on yield in most scenarios (Fig. 6J). The other two QTLs showed significant interaction with neither scenarios nor environmental variables (bin 8.08, 173.1 Mb, and bin 7.02, 97.1 Mb).

DISCUSSION

A Method for Classifying Genotypes and QTLs According to Environmental Scenarios, which Can Be Extrapolated to the Whole Maize-Cropping Area in Europe in Current or Future Conditions

Our approach for classifying environmental conditions sensed by plants in field experiments allowed identifying allelic effects in favorable scenarios or in stressing scenarios involving combinations of drought and heat stresses. Because maize is a C_4 species with limited effect of CO_2 on photosynthesis, these scenarios can apply to both current and future environmental conditions but with different frequencies. An important output was that an appreciable genetic variability was observed in stressing scenarios (e.g. 6 to 9 t ha^{-1} in scenarios with heat stress), thereby offering opportunities for breeding in these scenarios.

The classification of environment-related QTLs combined two methods, namely the test for a contrast in environmental scenarios and that for responses to individual environmental variables. The first method is original to our knowledge, while the second has already been used in other studies (Vargas et al., 2006; Boer et al., 2007; Malosetti et al., 2013) as proof of concept on smaller datasets. Classification in environmental scenarios can serve to estimate the comparative interest of any given genomic region, for any European region, by calculating the product of the mean allelic

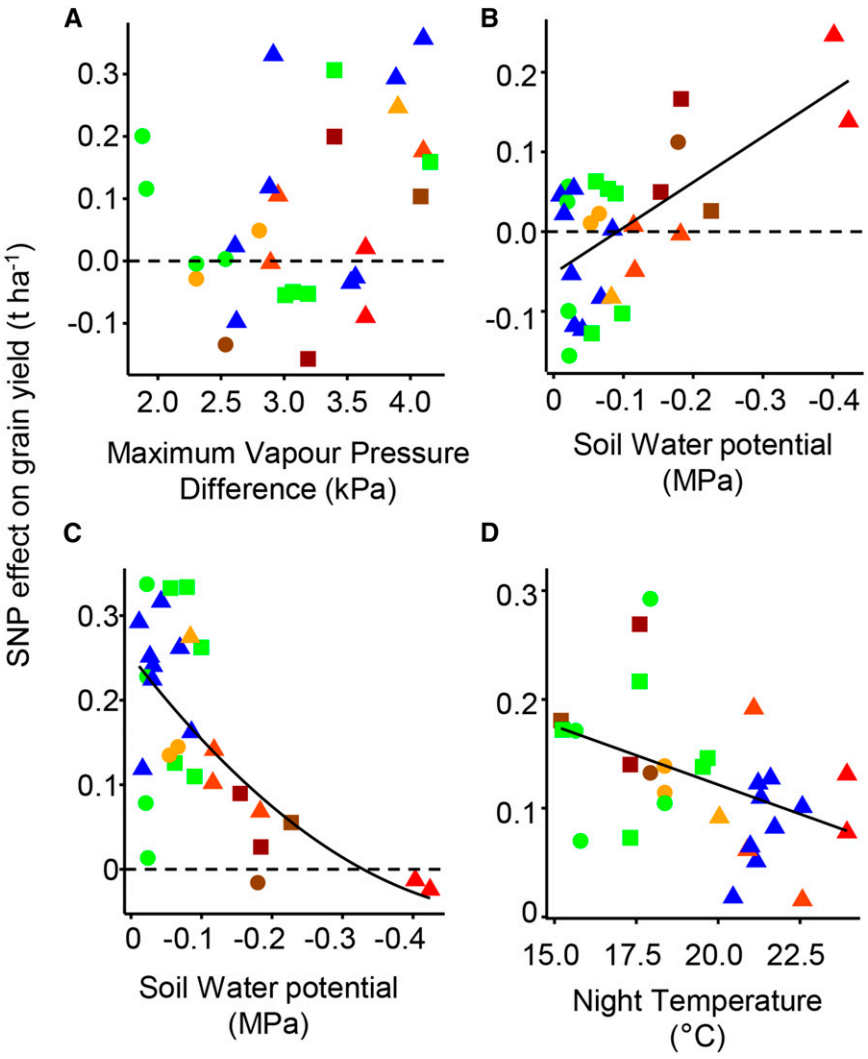

Figure 7. Allelic effects of QTLs on grain yield in relation to environmental variables. A, Allelic effect of QTL on chromosome 6.01 (19.0 Mb) as a function of VPD_{max}; B, allelic effect of QTL on chromosome 3.05 (150.4 Mb) as a function of soil water potential; C, allelic effect of QTL on chromosome 3.05 (159.0 Mb) as a function of soil water potential; D, allelic effect of QTL on chromosome 1.01 (2.4 Mb) as function of T_{night}. Colors and shapes of symbols as in Fig. 2. Allelic effects of grain yield (t ha^{-1}) were estimated using model M3. Environmental variables were averaged within a period of ± 10 $d_{20°C}$ around the flowering time of the reference hybrid. A to D, coefficients of Pearson's correlation were 0.32, 0.63, -0.64, and -0.42, respectively.

value in every scenario and the frequency of each scenario in the considered region. The method based on the regression of allelic effects with environmental variables can serve in marker assisted selection (MAS), by calculating the additive value of an allele as a function of environmental conditions. It can be extended to genomic selection (Jarquín et al., 2014).

This approach allows prediction of QTL effects in European regions to the difference of others: in particular, the classifications based on the datasets collected during experiments using either a hierarchical clustering of the G × E interaction (Moreau et al., 2004; Hageman et al., 2012) or composite environmental indices (Pidgeon et al., 2006; Bouffier et al., 2015). The difference between these approaches appears strikingly in the case of temperature. Our experiments were performed in sites and years classified as *Hot* in 76% of cases, versus only 2% in 52 European sites in the past 35 years by using the same thresholds. Although we cannot state whether this difference in frequency is due to climate change or to our sampling of sites and years, it is clear that the QTLs of tolerance for high temperatures identified in this study are relevant for future climatic scenarios, more than for current European climatic scenarios in the last 35 years. This could not have been detected with a classification based on the experimental dataset only. Similarly, Harrison et al. (2014) showed that any of the four water scenarios identified in Europe and used here for classifying experiments will probably be observed in the maize-producing area in 2050, although with markedly different frequencies. Hence, we think that the approach proposed here allows using field experiments performed in 2012 to 2013 for identifying genomic regions capable to reduce the impacts of climate change.

Modeling Allelic Effects as a Function of Environmental Conditions in Order to Identify QTLs for Heat and Drought Tolerance

The instability of QTL positions was similar to that observed in other multi-site experiments (Tuberosa

et al., 2002; Malosetti et al., 2008b; Bonneau et al., 2013). Nearly all QTLs identified here displayed a high and significant QTL × E interaction, with strong effects in a subset of experiments only. Overall, the QTL detection was satisfactory because the final set of QTLs of grain yield explained a high proportion of the genetic variance (79%), similar to that observed for more functional traits in maize, e.g. leaf elongation rate (74% in Reymond et al., 2003) or leaf architecture (83% in Tian et al., 2011).

The added value of our work was to model allelic effects according to environmental scenarios and variables, resulting in a predictive value of allelic effects instead of their instability in other studies.

(1) A first series of QTLs are involved in heat tolerance because allelic effects improved yield in hot experiments, but not in cooler experiments. Therefore, these QTLs may be considered to enhance tolerance to high temperatures. QTLs associated with maximum temperatures can affect yield through their effect on evaporative demand that lowers leaf water potential, or via heat stress per se, e.g. on pollen viability (Schoper et al., 1987). QTLs associated with night temperatures, some also observed by Hatfield et al. (2011), may act through carbon metabolism, in particular on the way in which starch is mobilized during the night (Stitt et al., 2010; Welch et al., 2010). The mechanisms underlying the responses of night and maximum temperatures are, therefore, markedly different. Candidate genes identified in QTL regions were involved in ABA signaling, thereby suggesting an effect via evaporative demand that decreases plant water potential.

(2) A second series of QTLs are involved in drought tolerance, with an improvement of yield in drought experiments, but not in well-watered conditions. Underlying mechanisms may act by improving hydraulic conductance of the root system (Chaumont and Tyerman, 2014) or by a reduction in the demand for transpiration by stomatal closure under high evaporative demand. Both processes maintain the growth of leaves or reproductive organs (Welcker et al., 2007; Oury et al., 2016a). The colocation of the QTL on bin 2.04, which showed negative effects in WW and positive effects in WD, with a gene of ABA biosynthesis whose effect is expected to present the same pattern, is an interesting example of how allelic effects in different scenarios can help suggesting a candidate gene among those harbored by the QTL.

(3) A third series of QTLs showed alleles associated with high performance in favorable conditions but higher sensitivity to temperature and water deficit. At least one of them (bin 3.05) was linked to a change in flowering time in our study, although it is not among best-known QTLs causing greatest effects on flowering time (Chardon et al., 2004; Salvi et al., 2007; Buckler et al., 2009). The low number of QTLs of flowering time is probably due to the restricted window of flowering time of our panel, thereby eliminating major actors of the genetic control of flowering time. Later flowering time causes an increased cumulated photosynthesis over the crop cycle, resulting in a higher potential yield in well-watered conditions. It also results in increased soil depletion in water deficit so flowering occurs when the soil is drier, thereby increasing grain abortion that counteracts the positive effect of later flowering time on cumulated photosynthesis. QTLs independent of flowering time harbored candidate genes involved in cell wall properties, cell cycle, or auxin signaling, expected to increase growth in favorable conditions.

Finally, it is noteworthy that one QTL only (Bin 8.06) increased yield regardless of the environmental conditions explored here, and that only two QTLs had allelic effects that could not be classified according to environmental scenarios. Hence, the vast majority of QTLs had context-dependent effects that were specific of precise scenarios and environmental conditions. We believe that this result reinforces the idea that breeding for tolerance to climate change will be more efficient if environmental scenarios during key phenological stages are explicitly taken into account for analyzing QTL effects (Tardieu, 2012). Furthermore, the response of allelic effects to environmental conditions across all experiments (regardless of QTL significance in individual experiments) has allowed identification of most likely candidate mechanisms and genes.

MATERIALS AND METHODS

Plant Material, Experiments, and Environmental Characterization

A maize hybrid population was generated by crossing a common flint parent (UH007) with 244 dent lines displaying a restricted flowering window. The resulting panel of hybrids had a flowering time within 7 d. Lines were genotyped using 50K Infinium HD Illumina array (Ganal et al., 2011) and a 600K Axiom Affymetrix array (Unterseer et al., 2014). After quality control, 515 081 polymorphic SNPs were retained for the analysis. All physical positions referred to hereafter are based on the B73 reference genome (Schnable et al., 2009) RefGen_V2.

The hybrid panel was evaluated in 29 experiments defined by a combination of year (2012 and/or 2013), site, and water regime. Sites were distributed on a West-East transect across Europe in France, south Germany, northern Italy, Hungary, and Romania at latitudes from 44° to 49° N compatible with the adaptation region of the panel (Supplemental Table S1). One experiment was performed in Chile (34° S). Experiments were designed as alpha-lattice designs with two and three replicates for watered and rain-fed regimes, respectively.

Light, air temperature, relative humidity (*RH*), and wind speed were measured every hour in each experiment at 2 m height over a reference grass canopy (Supplemental Fig. S7). Light was measured with PPFD sensors or pyranometers, depending on local practices; air temperature and *RH* were measured in ventilated shelters for calculation of vapor pressure deficit (VPD_{air}). Meteorological data obtained in each site were first converted to a unique set of variables with common units and then systematically checked for consistency and compared with those obtained in weather stations belonging to national/European networks. This led in some cases to new calibrations of the sensors used in local weather stations. Soil water potential was measured every day in the majority of fields (from every second hour to every fourth day) at 30, 60, and 90 cm depths in watered and rain-fed microplots sown with the reference hybrid B73 × UH007 with three and two replicates, respectively. Meristem temperature ($T_{meristem}$) was calculated every hour in each field, based on a simplified energy balance in which $T_{meristem}$ increases with light (import of energy) and decreases with VPD_{air} (increases transpiration, with an energy loss due to latent heat; Guilioni et al., 2000). A first equation was used until the beginning of stem elongation (eight-leaf stage), when $T_{meristem}$ is affected by the temperature of the upper soil layer:

$$T_{\text{meristem}} = 6.46 + 0.77\ T_{\text{air}} + 0.01\ R_{\text{g}} - 0.48\ W_{\text{soil}} - 0.22\ VPD_{air}$$

where T_{air} is air temperature at 2 m height (°C), R_g is global solar irradiance (W m^{-2}), and W_{soil} is soil water content (g g^{-1}) calculated via a water balance in the 0 to 3 cm soil layer. A second equation was used for later stages during which the apex is in the air:

$$T_{\text{meristem}} = 1.18 + T_{\text{air}} + 0.01\ R_{\text{g}} - 1.65\ VPD_{air}$$

Coefficients were determined with a linear model established on datasets collected in Mauguio (near Montpellier) and Grignon (near Paris). Resulting meristem temperatures were checked in independent datasets (Supplemental Fig. S8).

The leaf-to-air vapor pressure difference (*VPD*) was calculated from *RH* and T_{meristem}. Each day was characterized by the mean *VPD* for the three hours in the afternoon during which *VPD* was maximum (most often 12:00 to 15:00 solar time), referred to as VPD_{max}. Reference evapo-transpiration (ET_0) was calculated based on the Penman-Monteith equation as revised in the FAO-56 estimation (Allen et al., 1998). The progression of the crop cycle in each site was characterized via thermal time after emergence, expressed in equivalent days at 20°C ($d_{20°C}$; Parent et al., 2010).

Three scenarios of temperature were identified, depending on mean night and maximum temperature (T_{night} and T_{max}) over 20 $d_{20°C}$ encompassing flowering time of the reference hybrid. The threshold of T_{night} was set at 20°C and that of T_{max} at 3°C above 30°C, the temperature at which the rate of developmental processes decreases with temperature in maize (Parent et al., 2010, 2016). Meteorological values used for temperature scenarios in current conditions (1975–2010) were obtained from the AGRI4CAST database (Joint Research Centre [JRC], 2013) for 35 years in 55 European sites (Harrison et al., 2014). The same meteorological data have been used (Harrison et al. 2014) for generating scenarios of plant water status. Briefly, this involved the simulation of the supply/demand ratio for water with the APSIM model, resulting in 35 × 55 time courses that were subsequently clustered into four scenarios. The dataset that we have collected here includes time courses of soil water potential at three soil depths, thereby providing "real" environmental data. Conversely, the soil permanent characteristics necessary for running APSIM, such as the maximum soil water depletion at each depth, were not available to us. Hence, drought scenarios have been expressed based on measured soil water potential; they were also renamed here with more intuitive names. The limit of −0.1 MPa for mean soil water potential was appropriate for distinguishing WW and WD scenarios based on APSIM simulations carried out in fields for which the datasets were available for both modeling and direct measurement of soil water potential (data not shown).

Phenotypic Analyses

Grain yield and its components and male flowering dates were measured in each experiment. Grain yield was recorded simultaneously with the grain water content and adjusted to 15% moisture.

For each of the 29 experiments, genotypic means were calculated for each hybrid using a mixed model based on fixed hybrid and replicate effects, random spatial effects, and spatially correlated errors (Supplemental Methods S1) fitted with ASReml-R (Butler et al., 2009; R Core Team, 2013). The best linear unbiased estimations (BLUEs) of the genotypic means were then used for the rest of the analyses. The same model, but with random hybrid effects, was used to estimate variance components. Narrow-sense heritability was estimated at the plot level with a model assuming additive SNP effects using the R-package Heritability (Kruijer et al., 2015).

Multienvironment Analyses

We first fitted a mixed-model with random effects for genotype (*G*), genotype by location interaction ($G \times L$), genotype by year interaction ($G \times Y$), genotype by location by year interaction ($G \times L \times Y$), and experiment specific residual error variances (*E*):

$$Y = Env + PC + Env \times PC + \underline{G} + \underline{G \times L} + \underline{G \times Y} + \underline{G \times L \times Y} + \underline{E} \qquad M1$$

where *Y* is the vector of all phenotypic observations, *Env* represents fixed experiment-specific means, and *PC* denotes a fixed term that refers to the first 10 principal components of the kinship matrix used to correct for population structure (Supplemental Methods S2). Following van Eeuwijk et al. (2010), the interaction between experiment and *PC* was also taken into account ($Env \times PC$). The variance components of random terms were extracted and the standard deviations were expressed as a percentage of the general phenotypic mean (Gelman, 2005). Any effect in the model can contribute to differences in phenotype for individual genotypes within a range of ± twice the SD. This range was also expressed as a percentage of the general mean.

Next, we extended model M1 with a random effect accounting for the interaction between genotype and environmental classification ($G \times EC$):

$$Y = Env + PC + Env \times PC + \underline{G} + \underline{G \times EC} + \underline{G \times L} + \underline{G \times Y} + \underline{G \times L \times Y} + \underline{E} \qquad M2$$

GWAS Analysis

GWAS was first performed on individual traits for each single experiment (SE) using the single locus mixed model

$$Y = \mu + X\beta + G + E$$

where *Y* is the vector of phenotypic values, μ the overall mean, *X* is the vector of SNP scores, β is the additive effect, and *G* and *E* represent random polygenic and residual effects. As in Rincent et al. (2014), the variance-covariance matrix of *G* was determined by a genetic relatedness (or kinship) matrix, derived from all SNPs except those on the chromosome containing the SNP being tested (Supplemental Methods S2). The SNP effects β were estimated by generalized least squares, and their significance (H_0: $\beta = 0$) tested with an F-statistic. Analyses were performed with FaST-LMM v2.07 (Lippert et al., 2011).

Subsequently, we performed single locus multienvironment (ME) GWAS with the same dataset (Supplemental Methods S3). To overcome the computational burden posed by the large number of experiments, we combined the diagonalization approach of Zhou and Stephens (2014) with the factor analytic models commonly used in multitrait and multienvironment QTL-mapping in experimental populations (Boer et al., 2007; Malosetti et al., 2008a).

An initial set of SNPs was selected based on the joint result of single locus SE and ME GWAS by including all SNPs with $-\log_{10}$(*P* value) larger than five. This initial screening for candidate QTLs was deliberately performed with a relatively mild significance threshold to ensure that we would not miss potentially interesting SNPs. The protection against false positives was ensured by backward elimination of candidate QTLs from a multilocus ME mixed model. Physical positions of significant SNPs were projected on the consensus genetic map for Dent genetic material (Giraud et al., 2014). Candidate SNPs distant less than 0.1 cM were considered as belonging to a common QTL, described via the most significant SNP in the QTL and the interval between all SNPs belonging to the QTL.

Dissection of G × E and QTL × E

To investigate the structure of G × E and QTL × E effects, we fitted a ME model with multiple QTLs:

$$Y = Env + PC + Env \times PC + \sum_{q \in Q} QTL_q^{Env} + \underline{G} + \underline{G \times EC} + \underline{G \times L} + \underline{G \times Y} + \underline{G \times L \times Y} + \underline{E} \qquad M3$$

with $QTL_q^{Env} = QTL_q + (QTL \times Env)_q$. We have fitted environment-specific QTL effects that are the sum of a QTL main effect and a QTL by environment interaction term. Model M3 extends model M2 with a final set of QTLs called *Q*. The final composition of *Q* was determined by first including the complete set of candidate QTLs, and then performing backward elimination based on the Wald tests for the individual terms QTL_q^{Env}, removing at each step the least significant QTL, until all QTLs were significant at 0.01 (Supplemental Methods S4). To assess the amount of genetic (co)variance explained by the QTLs, we compared the estimated variance components in M3 with those obtained from M2. A short description of each model is presented in Supplemental Table S9.

For each of the QTLs in model M3, the part due to $(QTL \times Env)_q$ was dissected by modeling this interaction as the sum of index-specific effects and a residual term representing QTL×E variation not captured by the environmental index:

$$(QTL \times Env)_q = (QTL_q^{Sensitivity} \times index) + QTL_q^{Residual}$$

Substituting this in model M3 gave an equivalent model, but also gave a Wald test for the significance of the interaction $(QTL_q^{Sensitivity} \times index)$ that could be either a test for contrast in scenarios (e.g. test for QTL × EC) or a continuous environmental variable (e.g. QTL × T_{max}).

Allelic effects of all candidate QTLs were extracted from model M3. When no indication is provided, a positive effect indicates that the reference hybrid allele increased the trait value, while a negative effect indicates that the alternative allele increased the trait value (Supplemental Methods S5).

Candidate Genes

Each identified region was queried in the maize 5b annotation file ZmB73_5b_FGS_info.txt downloaded from maizesequence.org using a custom Perl script. It was functionally annotated using the MapMan annotation and cross-referenced to Affymetrix microarray probes using the publicly available Affymetrix information file Release 35. To this aim, data from Zheng et al. (2010) was obtained from GEO and analyzed using ROBINA (Lohse et al., 2012), and RNASeq results from the supplement of Liu et al. (2015) were integrated using a custom script.

Supplemental Data

The following supplemental materials are available.

Supplemental Figure S1. Principal component analysis on the weather variables.

Supplemental Figure S2. Variability of grain yield per experiment.

Supplemental Figure S3. Genotypic variability of grain yield for all hybrids in the six environmental scenarios.

Supplemental Figure S4. Relationship between grain yield and grain number (A) and between grain size and grain number (B) for the whole panel of hybrids.

Supplemental Figure S5. Final set of significant QTLs for grain number (A) and size (B) in the different experiments.

Supplemental Figure S6. Heatmap of the allelic effect the 36 QTLs of grain yield per environmental scenario.

Supplemental Figure S7. Time courses of weather variables in one location (Gai13).

Supplemental Figure S8. Comparison of estimated and observed meristem temperature.

Supplemental Table S1. Weather variables, grain yield and yield components over the network of experiments.

Supplemental Table S2. Correlations between environmental variables, grain yield, and its components.

Supplemental Table S3. Genotypic variability of grain yield for all hybrids in the six environmental scenarios.

Supplemental Table S4. Statistical indicators of the genetic variability for grain yield (A), grain number (B), and grain size (C) in individual experiments.

Supplemental Table S5. Variance components of the different models for grain number (A) and grain size (B).

Supplemental Table S6. Dissection of QTL × Env on the 48 QTLs of grain yield (t ha^{-1}).

Supplemental Table S7. Final set of QTLs for grain number (A and B, nb m^{-2}) and grain size (C and D, mg) and QTL × E tests.

Supplemental Table S8. Candidate genes found in QTL regions.

Supplemental Table S9. Short description of statistical models.

Supplemental Methods S1. Additional methodological details on the single environments phenotypic analysis.

Supplemental Methods S2. Additional methodological details on the estimates of genetic relatedness and the use of marker information.

Supplemental Methods S3. Additional methodological details on the ME GWAS.

Supplemental Methods S4. Additional methodological details on the ME multi-QTL model.

Supplemental Methods S5. Additional methodological details on the dissection of G × E and QTL × E.

ACKNOWLEDGMENTS

We are grateful to partners of the CornFed project, Univ. Hohenheim (Germany), CSIC (Spain), CRAG (Spain), MTA ATK (Hungary), NCRPIS (USA), CRB Maize (France), and CRA-MAC (Italy) who contributed genetic material. We are grateful to key partners from the field: Pierre Dubreuil, Cécile Richard, Jérémy Lopez (Biogemma), Tamás Spitkó (MTA ATK), Therese Welz (KWS), Franco Tanzi, Ferenc Racz, Vincent Schlegel (Syngenta), and Maria Angela Canè (UNIBO). We also acknowledge Delphine Madur and Valérie Combes (INRA) for their contribution to the genotypic analysis and Axel Nagel (MPI) for data management.

Received April 22, 2016; accepted July 12, 2016; published July 19, 2016.

LITERATURE CITED

Allen RG, Pereira LS, Raes D, Smith M (1998) Crop evapotranspiration: guidelines for computing crop water requirements. Food and Agriculture Organization of the United Nations, Rome

Basu D, Tian L, Debrosse T, Poirier E, Emch K, Herock H, Travers A, Showalter AM (2016) Glycosylation of a Fasciclin-Like Arabinogalactan-Protein (SOS5) Mediates Root Growth and Seed Mucilage Adherence via a Cell Wall Receptor-Like Kinase (FEI1/FEI2) Pathway in Arabidopsis. PLoS One **11:** e0145092

Bishop KA, Betzelberger AM, Long SP, Ainsworth EA (2015) Is there potential to adapt soybean (*Glycine max* Merr.) to future [CO_2]? An analysis of the yield response of 18 genotypes in free-air CO_2 enrichment: Variation in soybean response to elevated. CO2. Plant Cell Environ **38:** 1765–1774

Boer MP, Wright D, Feng L, Podlich DW, Luo L, Cooper M, van Eeuwijk FA (2007) A mixed-model quantitative trait loci (QTL) analysis for multiple-environment trial data using environmental covariables for QTL-by-environment interactions, with an example in maize. Genetics **177:** 1801–1813

Bonneau J, Taylor J, Parent B, Bennett D, Reynolds M, Feuillet C, Langridge P, Mather D (2013) Multi-environment analysis and improved mapping of a yield-related QTL on chromosome 3B of wheat. Theor Appl Genet **126:** 747–761

Bouffier B, Derory J, Murigneux A, Reynolds M, Le Gouis J (2015) Clustering of Environmental Parameters Discriminates Drought and Heat Stress Bread Wheat Trials. Agron J **107:** 1489–1503

Buckler ES, Holland JB, Bradbury PJ, Acharya CB, Brown PJ, Browne C, Ersoz E, Flint-Garcia S, Garcia A, Glaubitz JC, Goodman MM, Harjes C, et al (2009) The genetic architecture of maize flowering time. Science **325:** 714–718

Butler DG, Cullis BR, Gilmour AR, Gogel BJ (2009) ASReml-R User Guide Release 3.0.

Canel C, Bailey-Serres JN, Roose ML (1995) Pummelo fruit transcript homologous to ripening-induced genes. Plant Physiol **108:** 1323–1324

Chapman SC, Cooper M, Hammer GL, Butler DG (2000) Genotype by environment interactions affecting grain sorghum. II. Frequencies of different seasonal patterns of drought stress are related to location effects on hybrid yields. Aust J Agric Res **51:** 209–222

Chardon F, Virlon B, Moreau L, Falque M, Joets J, Decousset L, Murigneux A, Charcosset A (2004) Genetic architecture of flowering time in maize as inferred from quantitative trait loci meta-analysis and synteny conservation with the rice genome. Genetics **168:** 2169–2185

Chaumont F, Tyerman SD (2014) Aquaporins: highly regulated channels controlling plant water relations. Plant Physiol **164:** 1600–1618

Chenu K, Cooper M, Hammer GL, Mathews KL, Dreccer MF, Chapman SC (2011) Environment characterization as an aid to wheat improvement: interpreting genotype-environment interactions by modelling water-deficit patterns in North-Eastern Australia. J Exp Bot **62:** 1743–1755

Collins NC, Tardieu F, Tuberosa R (2008) Quantitative trait loci and crop performance under abiotic stress: where do we stand? Plant Physiol **147:** 469–486

van Eeuwijk FA, Bink MC, Chenu K, Chapman SC (2010) Detection and use of QTL for complex traits in multiple environments. Curr Opin Plant Biol **13:** 193–205

Fiorani F, Schurr U (2013) Future scenarios for plant phenotyping. Annu Rev Plant Biol **64:** 267–291

Ganal MW, Durstewitz G, Polley A, Bérard A, Buckler ES, Charcosset A, Clarke JD, Graner E-M, Hansen M, Joets J, Le Paslier MC, McMullen MD, et al (2011) A large maize (*Zea mays* L.) SNP genotyping array: development and germplasm genotyping, and genetic mapping to compare with the B73 reference genome. PLoS One **6:** e28334

Gelman A (2005) Analysis of variance - why it is more important than ever. Ann Stat **33:** 1–53

Giraud H, Lehermeier C, Bauer E, Falque M, Segura V, Bauland C, Camisan C, Campo L, Meyer N, Ranc N, Schipprack W, Flament P, et al (2014) Linkage disequilibrium with linkage analysis of multiline crosses reveals different multiallelic QTL for hybrid performance in the flint and dent heterotic groups of maize. Genetics **198:** 1717–1734

Giuliani S, Sanguineti MC, Tuberosa R, Bellotti M, Salvi S, Landi P (2005) *Root-ABA1*, a major constitutive QTL, affects maize root architecture and leaf ABA concentration at different water regimes. J Exp Bot **56:** 3061–3070

Guilioni L, Cellier P, Ruget F, Nicoullaud B, Bonhomme R (2000) A model to estimate the temperature of a maize apex from meteorological data. Agric Meteorol **100:** 213–230

Hageman JA, Malosetti M, van Eeuwijk FA (2012) Two-mode clustering of genotype by trait and genotype by environment data. Euphytica **183:** 349–359

Harrison MT, Tardieu F, Dong Z, Messina CD, Hammer GL (2014) Characterizing drought stress and trait influence on maize yield under current and future conditions. Glob Change Biol **20:** 867–878

Hatfield JL, Boote KJ, Kimball BA, Ziska LH, Izaurralde RC, Ort D, Thomson AM, Wolfe D (2011) Climate Impacts on Agriculture: Implications for Crop Production. Agron J **103:** 351–370

IPCC (2014) Climate Change 2014: Synthesis Report. Contribution of Working Groups I, II and III to the Fifth Assessment Report of the Intergovernmental Panel on Climate Change. Core Writing Team, RK Pachauri, LA Meyer IPCC, Geneva, Switzerland

Jarquín D, Crossa J, Lacaze X, Du Cheyron P, Daucourt J, Lorgeou J, Piraux F, Guerreiro L, Pérez P, Calus M, Burgueño J, de los Campos G (2014) A reaction norm model for genomic selection using high-dimensional genomic and environmental data. Theor Appl Genet **127:** 595–607

K MJ, Laxmi A (2014) DUF581 is plant specific FCS-like zinc finger involved in protein-protein interaction. PLoS One **9:** e99074

Kruijer W, Boer MP, Malosetti M, Flood PJ, Engel B, Kooke R, Keurentjes JJB, van Eeuwijk FA (2015) Marker-based estimation of heritability in immortal populations. Genetics **199:** 379–398

Langridge P, Fleury D (2011) Making the most of 'omics' for crop breeding. Trends Biotechnol **29:** 33–40

Lippert C, Listgarten J, Liu Y, Kadie CM, Davidson RI, Heckerman D (2011) FaST linear mixed models for genome-wide association studies. Nat Methods **8:** 833–835

Liu Y, Zhou M, Gao Z, Ren W, Yang F, He H, Zhao J (2015) RNA-Seq Analysis Reveals MAPKKK Family Members Related to Drought Tolerance in Maize. PLoS One **10:** e0143128

Lobell DB, Schlenker W, Costa-Roberts J (2011) Climate trends and global crop production since 1980. Science **333:** 616–620

Lohse M, Bolger AM, Nagel A, Fernie AR, Lunn JE, Stitt M, Usadel B (2012) RobiNA: a user-friendly, integrated software solution for RNA-Seq-based transcriptomics. Nucleic Acids Res **40:** W622-7

Maccaferri M, El-Feki W, Nazemi G, Salvi S, Canè MA, Colalongo MC, Stefanelli S, Tuberosa R (2016) Prioritizing quantitative trait loci for root system architecture in tetraploid wheat. J Exp Bot **67:** 1161–1178

Maccaferri M, Sanguineti MC, Corneti S, Ortega JLA, Salem MB, Bort J, DeAmbrogio E, del Moral LFG, Demontis A, El-Ahmed A, Maalouf F, Machlab H, et al (2008) Quantitative trait loci for grain yield and adaptation of durum wheat (*Triticum durum* Desf.) across a wide range of water availability. Genetics **178:** 489–511

Malosetti M, Ribaut J-M, van Eeuwijk FA (2013) The statistical analysis of multi-environment data: modeling genotype-by-environment interaction and its genetic basis. Front Physiol **4:** 44

Malosetti M, Ribaut JM, Vargas M, Crossa J, van Eeuwijk FA (2008a) A multi-trait multi-environment QTL mixed model with an application to drought and nitrogen stress trials in maize (*Zea mays* L.). Euphytica **161:** 241–257

Malosetti M, Ribaut JM, Vargas M, Crossa J, van Eeuwijk FA (2008b) A multi-trait multi-environment QTL mixed model with an application to drought and nitrogen stress trials in maize (*Zea mays* L.). Euphytica **161:** 241–257

Moreau L, Charcosset A, Gallais A (2004) Use of trial clustering to study QTL x environment effects for grain yield and related traits in maize. Theor Appl Genet **110:** 92–105

Oury V, Caldeira CF, Prodhomme D, Pichon J-P, Gibon Y, Tardieu F, Turc O (2016a) Is change in ovary carbon status a cause or a consequence of maize ovary abortion in water deficit during flowering? Plant Physiol **171:** 997–1008

Oury V, Tardieu F, Turc O (2016b) Ovary apical abortion under water deficit is caused by changes in sequential development of ovaries and in silk growth rate in maize. Plant Physiol **171:** 986–996

Padmanabhan V, Dias DM, Newton RJ (1997) Expression analysis of a gene family in loblolly pine (*Pinus taeda* L.) induced by water deficit stress. Plant Mol Biol **35:** 801–807

Parent B, Turc O, Gibon Y, Stitt M, Tardieu F (2010) Modelling temperature-compensated physiological rates, based on the co-ordination of responses to temperature of developmental processes. J Exp Bot **61:** 2057–2069

Parent B, Vile D, Violle C, Tardieu F (2016) Towards parsimonious eco-physiological models that bridge ecology and agronomy. New Phytol **210:** 380–382

Pidgeon JD, Ober ES, Qi A, Clark CJA, Royal A, Jaggard KW (2006) Using multi-environment sugar beet variety trials to screen for drought tolerance. Field Crops Res **95:** 268–279

R Core Team (2013) R: A Language and Environment for Statistical Computing. R Foundation for Statistical Computing, Vienna, Austria

Reymond M, Muller B, Leonardi A, Charcosset A, Tardieu F (2003) Combining quantitative trait Loci analysis and an ecophysiological model to analyze the genetic variability of the responses of maize leaf growth to temperature and water deficit. Plant Physiol **131:** 664–675

Rincent R, Moreau L, Monod H, Kuhn E, Melchinger AE, Malvar RA, Moreno-Gonzalez J, Nicolas S, Madur D, Combes V, Dumas F, Altmann T, et al (2014) Recovering power in association mapping panels with variable levels of linkage disequilibrium. Genetics **197:** 375–387

Salekdeh GH, Reynolds M, Bennett J, Boyer J (2009) Conceptual framework for drought phenotyping during molecular breeding. Trends Plant Sci **14:** 488–496

Salvi S, Corneti S, Bellotti M, Carraro N, Sanguineti MC, Castelletti S, Tuberosa R (2011) Genetic dissection of maize phenology using an intraspecific introgression library. BMC Plant Biol **11:** 4

Salvi S, Sponza G, Morgante M, Tomes D, Niu X, Fengler KA, Meeley R, Ananiev EV, Svitashev S, Bruggemann E, Li B, Hainey CF, et al (2007) Conserved noncoding genomic sequences associated with a flowering-time quantitative trait locus in maize. Proc Natl Acad Sci USA **104:** 11376–11381

Schnable PS, Ware D, Fulton RS, Stein JC, Wei F, Pasternak S, Liang C, Zhang J, Fulton L, Graves TA, Minx P, Reily AD, et al (2009) The B73 maize genome: complexity, diversity, and dynamics. Science **326:** 1112–1115

Schoper JB, Lambert RJ, Vasilas BL, Westgate ME (1987) Plant factors controlling seed set in maize : the influence of silk, pollen, and ear-leaf water status and tassel heat treatment at pollination. Plant Physiol **83:** 121–125

Semenov M, Stratonovitch P (2010) Use of multi-model ensembles from global climate models for assessment of climate change impacts. Clim Res **41:** 1–14

Stitt M, Lunn J, Usadel B (2010) Arabidopsis and primary photosynthetic metabolism - more than the icing on the cake. Plant J **61:** 1067–1091

Tardieu F (2012) Any trait or trait-related allele can confer drought tolerance: just design the right drought scenario. J Exp Bot **63:** 25–31

Tardieu F, Parent B, Simonneau T (2010) Control of leaf growth by abscisic acid: hydraulic or non-hydraulic processes? Plant Cell Environ **33:** 636–647

Tardieu F, Tuberosa R (2010) Dissection and modelling of abiotic stress tolerance in plants. Curr Opin Plant Biol **13:** 206–212

Tester M, Langridge P (2010) Breeding technologies to increase crop production in a changing world. Science **327:** 818–822

Tian F, Bradbury PJ, Brown PJ, Hung H, Sun Q, Flint-Garcia S, Rocheford TR, McMullen MD, Holland JB, Buckler ES (2011) Genome-wide association study of leaf architecture in the maize nested association mapping population. Nat Genet **43:** 159–162

Tuberosa R, Salvi S, Sanguineti MC, Landi P, Maccaferri M, Conti S (2002) Mapping QTLs regulating morpho-physiological traits and yield: case studies, shortcomings and perspectives in drought-stressed maize. Ann Bot (Lond) **89:** 941–963

Unterseer S, Bauer E, Haberer G, Seidel M, Knaak C, Ouzunova M, Meitinger T, Strom TM, Fries R, Pausch H, Bertani C, Davassi A, et al (2014) A powerful tool for genome analysis in maize: development and evaluation of the high density 600 k SNP genotyping array. BMC Genomics **15:** 823 10.1186/1471-2164-15-823

Van Genuchten MT (1980) A closed-form equation for predicting the hydraulic conductivity of unsaturated soils. Soil Sci Soc Am **44:** 892–898

Vargas M, van Eeuwijk FA, Crossa J, Ribaut J-M (2006) Mapping QTLs and QTL x environment interaction for CIMMYT maize drought stress program using factorial regression and partial least squares methods. Theor Appl Genet **112:** 1009–1023

Venancio TM, Aravind L (2010) CYSTM, a novel cysteine-rich transmembrane module with a role in stress tolerance across eukaryotes. Bioinformatics **26:** 149–152

Welch JR, Vincent JR, Auffhammer M, Moya PF, Dobermann A, Dawe D (2010) Rice yields in tropical/subtropical Asia exhibit large but opposing sensitivities to minimum and maximum temperatures. Proc Natl Acad Sci USA **107:** 14562–14567

Welcker C, Boussuge B, Bencivenni C, Ribaut J-M, Tardieu F (2007) Are source and sink strengths genetically linked in maize plants subjected to water deficit? A QTL study of the responses of leaf growth and of Anthesis-Silking Interval to water deficit. J Exp Bot **58:** 339–349

Zheng J, Fu J, Gou M, Huai J, Liu Y, Jian M, Huang Q, Guo X, Dong Z, Wang H, Wang G (2010) Genome-wide transcriptome analysis of two maize inbred lines under drought stress. Plant Mol Biol **72:** 407–421

Zhou X, Stephens M (2014) Efficient multivariate linear mixed model algorithms for genome-wide association studies. Nat Methods **11:** 407–409

Zhu C, Gore M, Buckler ES, Yu J (2008) Status and Prospects of Association Mapping in Plants. Plant Genome J **1:** 5